PIIT JOURNAL OF MECHANICAL ENGINEERING

PCE
PILLAI COLLEGE OF ENGINEERING
ISSN 2277-5951

Year | 2017

CONTENTS

EDITORIAL

Modeling Fabrication and Testing of Artificial Gecko adhesion using multi layer fibrillar structure

Ameya P. Nijasure, Priam V. Pillai

Department of Mechanical Engineering, Pillai Collage of Engineering
New Panvel, Raigad, India.
napradeep@mes.ac.in, ppillai@mes.ac.in,

Abstract- The idea of designing a micro level artificial gecko adhesive structure is inspired from ability of geckos to climb any surface. Gecko can climb any rough or smooth surface because of its hierarchical structure present on feet which functions as a smart adhesive [1]. The key parameter that affects gecko adhesion are pattern periodicity of a synthetic setae, hierarchical structure, length, diameter, angle, size, stiffness of end tips and flexibility of a base [2]. The design and fabrication of number of single and multi-level hierarchical pattern were performed. CO2 LASER cutting machine having power of 60 W is used to manufacture moulds. The mould is fabricated from methyl methacrylate sheets of different thickness 3 mm to 10 mm. Liquid silicone polymer PDMS is used as a cast material. Various patterns having dimensionsupto200 micrometer with different tip shapes and geometries were fabricated. For single level patterns like dense pattern, mushroom shape pattern and wedge pattern (lamellar structure) were fabricated. Attempts were made to design and fabricate Multi-level hierarchical structure patterns that mimics gecko like foot structure. These micro level artificial gecko structure have large scope of applications such as climbing robots, non-sticky adhesion tapes, military surveillance and even medical applications.

Keywords- LASER cutting, artificial gecko, Adhesion, Setae, Spatula.

I. Introduction

A number of researchers studied gecko adhesion using various theoretical and experimental techniques to understand frictional adhesion properties and mechanism of gecko feet, hairs and setae in order to mimic the gecko feet as strong, non-sticky and self-cleaning adhesion. The conventional adhesives like Pressure Sensitive Adhesives (PSAs) are soft and sticky to make continuous contact with the surface. PSAs have major effects of fouling, degrade and accidentally adhere any surface when not required. Whereas compared to PSAs artificial gecko adhesives are non-tacky, self-cleaning, easy to attach and detach. The ability of geckos to climb any rough or smooth surface at any angle inspired researchers to develop non-tacky pads for vertical climbing robots and many such applications.

The principle behind geckos extraordinary adhesion is van der waals forces of molecular attraction. Due to hierarchical fibrillar structure this weak van der waals force get converted into strong bond because of more than million number of point of contacts. The advantage of designing fibrillar adhesive structure when compared with flat structure is that each fiber deform independently, which makes sure that each fiber reaches deeper in case of rough surface to achieve clean contact [8]. The key parameter that plays important role in gecko adhesion are pattern periodicity of a synthetic setae, hierarchical structure, length, diameter, angle, size, stiffness of end tips and flexibility of a base.

Each five-toed foot of the gecko has about 500,000 foot-hairs called setae a uniformly distributed array each about 110μm in length and 4.2μm diameter. Further it is divided in to spatulae a thin stalk with triangular shape tiny end of 0.2μm length and width. [1].

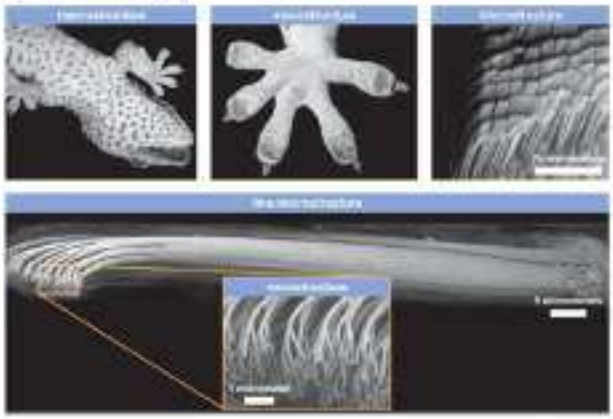

Figure 1. Gecko foot structure [1]

In the developments of synthetic setae, polymers like polyimide, polypropylene and polydimethylsiloxane (PDMS) are frequently used since they are flexible and easily fabricated. Later, as nanotechnology developed, carbon nanotubes are preferred and used in most recent projects [6]. Carbon nanotubes have both extraordinary strength and flexibility, as well as good electrical properties. Gecko adhesion widely dependent on geometry of gecko feet and adhesive material properties.

Gecko setal arrays have excellent ability of self-cleaning. Also they are non-sticky which has considerably wider application potential over pressure sensitive adhesives in

several areas such as robotics for rescue and detection, chemical sensing, space position and medical application. Although Gecko adhesives are widely used in robotics application it can be also used into industry/manufacturing application where residue free and releasable tape is required. From the introduction of nanotechnology in gecko adhesion it can be directly applied to surface, which could replace screws, glues and interlocking surface like Velcros in many assembly applications such as in automotive, mobile phones etc [9]. Gecko inspired dry adhesives can be used in bio-medical application such as endoscopy and tissue adhesion. However material selected for synthetic satae for such application must be non-toxic and non-irritating. Other applications include micro mechanical and electrical systems (MEMS), wafer alignment, micro-manipulation [2].

II. Design and Fabrication

CO_2 LASER cutting machine having power of 60 W is used to manufacture moulds. The parameters which affects LASER cutting are speed and power. Cutting depth and quality are determined by a combination of power and speed. Slower speeds at higher power will produce deeper cuts. Whereas higher speeds at lower power will produce more shallow cuts. With various combinations of these parameter fabrication of different types of moulds done. The mould is fabricated from methyl methacrylate sheet of 3 mm to 8 mm thickness.

Liquid silicone polymer PDMS having tensile strength of 1.65 MPa and elongation at break is 250% is used. This method of fabrication is simple and low cost.

Taking reference from research papers various types and shapes of fibillar structures like single level, multi-level and lamellar etc. are chosen. Keeping area of contact as a preference sample size kept constant to 20mm X 20mm for all types of patterns. Fabrication of dense pattern with base diameter approximately 200 micron and height of 1mm is done shown in fig 2 (a).

Similarly considering lamellar pattern fabricated wedge pattern with base dimension as 200 micron and height up to 400 micron. The challenge in designing wedge pattern is making one edge of wedge inclined as our laser angle and bed base is fixed workpiece made inclined at 10 degree shown in fig 2 (b) [3].

While laser cutting various materials like wood, acrylic, paper etc. also trial cutting on plastic sheets were performed. So while laser cutting a plastic sheet it is found that tip like structure on end of each hair because of tar (sudden vaporization due to high temperature of LASER) is formed which can be used as a contact area for adhesion.

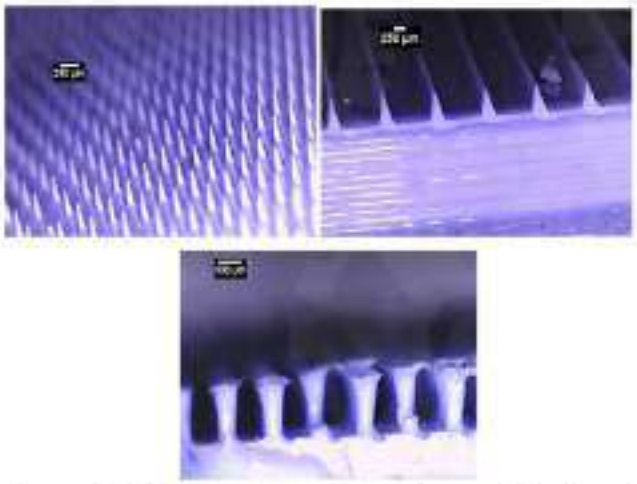

Figure 2. a) Dense pattern using various combinations of speed and power as parameters. b) Wedge shape pattern using inclined sample c) Plastic mould pattern using plastic sheet as a raw material.

Various attempts for fabrication of two level fibillar structure were performed using LASER cutting. The challenge in fabricating such multi-level structure is integrated geometry and consistent pattern over a surface. Fabrication of some multi-level fibillar structure shown in fig 2(a and b).

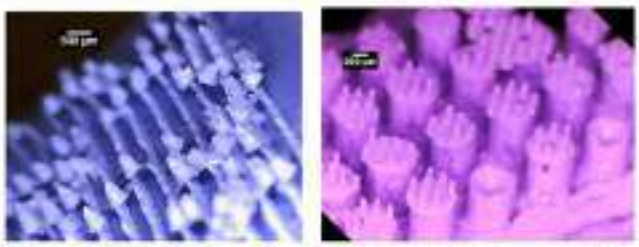

Figure 3. a) Mushroom head pattern using Laser cutting and engraving b) Multi-level pattern using multi-level moulding process

From reference to Michel P. Murphy, Seok kim "enhanced adhesion by gecko inspired hierarchical fibillar adhesives" multi-level micro scale structure results in significant decrease in adhesion [4].

III. Result and Desscusion

Initialtestswereperformedonthesamplestodeterminecoefficie ntofadhesion.therelationshipofshearforcetonormalforceisaconst antvaluesstatedbyAmonton'sfirstlaw.when setae are dragged across a surface they exhibit friction typically called Amontos friction. The coefficient of adhesion can be expressed as

$$\mu = \frac{F_N}{F_T}$$

Where μ = Coefficient of Adhesion
F_N = Normal force
F_T = Tangent force

Tests were performed on three samples to determine coefficient of adhesion i.e. flat pattern (no geometry), wedge

pattern and plastic mould pattern. In Dense pattern sharp tips were observed because of the manufacturing process (LASER cutting). As tip dimension is smaller it will not sustain load applied hence not considered in testing. Also multi-level pattern fabricated using LASER cutting method is not consistent over the surface.

Preload (gms)	Coefficient of adhesion(μ)		
	Flat sample	Mushroom head pattern	Wedge pattern
3	3.17	2.17	2.87
13	1.42	0.96	1.65
23	1.50	0.76	2.07
33	1.25	0.70	2.34
43	1.05	0.65	1.87
53	0.90	0.59	1.65
63	0.80	0.55	1.54

Table 1. Calculations for Coefficient of adhesion

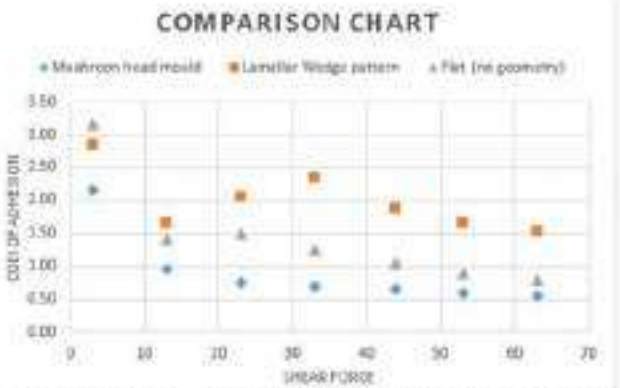

Graph 1. Graph - preload against coeificient of adhesion for wedge, flat and plastic mould pattern

From above graph and result table wedge pattern is having more consistent coefficient of adhesion over a large range when pre load is increased.

IV. CONCLUSION

Wedge shaped lamellar pattern, dense pattern and plastic mould pattern is fabricated using laser cutting process. From above result for a micro level fibillar structure in basic testing coefficient of adhesion μ can be determined up to 2.83. Whereas the adhesion coefficient of real gecko setae is typically 8~16[7].

Further tests can be performed on wedge pattern and more geometry shapes for a better adhesion. Laser cutting is having a limitation of least dimension approx. 150 micron so it cannot be used for fabricating a multi-level structure for better and accurate results.

V. REFERENCES

[1] Kellar Autumn and Nick Gravish. Gecko adhesion: evolutionary nanotechnology. Philosophical Transactions of the Royal Society of London A: Mathematical, Physical and Engineering Sciences, 366(1870):1575–1590, 2008.

[2] Yang Li, Hao Zhang, Zhendong Dai, Geza Toth, Krisztian Kordas, Yagang Yao, Yongyi Zhang, and Qingwen Li. Gecko foot mimetic carbon nanotube patterned adhesive surfaces.

[3] Aaron Parness, Daniel Soto, No'e Esparza, Nick Gravish, Matt Wilkinson, Kellar Autumn, and Mark Cutkosky. A microfabricated wedge-shaped adhesive array displaying gecko-like dynamic adhesion, directionality and long lifetime. Journal of the Royal Society Interface, pages rsif–2009, 2009.

[4] Michael P Murphy, Seok Kim, and Metin Sitti. Enhanced adhesion by gecko-inspired hierarchical fibrillar adhesives. ACS applied materials & interfaces, 1(4):849–855, 2009.

[5] Pramod Murali Mohan, Sagar Ayare, and Esh Pin. Gecko stick.

[6] Michael P Murphy, Seok Kim, and Metin Sitti. Enhanced adhesion by gecko-inspired hierarchical fibrillar adhesives. ACS applied materials & interfaces, 1(4):849–855, 2009.

[7] Synthetic setae, 2015. https://en.wikipedia.org/wiki/Synthetic_setae

Performance Analysis of Crash box in Automobiles

Komal A Kadam

Department Of Mechanical Engineering
Pillai College of Engineering,
New Panvel,India
kadam@mes.ac.in

Dr.Vinayak H Khatawate

Department Of Mechanical Engineering,
D J Sanghvi College of Engineering,
Vile Parle, Mumbai, India
vinayakhk@gmail.com

***Abstract*- For protecting the occupants in the car many times the safety features are of prime importance. The crash box of the automobile is also one of the important safety feature which absorbs initial impact. The parts such as fender, hood, intercooler and radiator which are expensive to repair are protected with the help of crash box. While moving car has kinetic energy and becomes zero when it comes to stop. For minimizing the risk of the fatal or serious injury to the occupants in the car, crash box is necessary. Kinetic energy of the car is absorbed by crash box, so as to reduce risk of injury and death of occupants. As there were many accidents and collisions, to avoid risks the concept of energy absorption component i.e. crash box came into existence. Crash box analysis focused on the study of structural configurations of crash box. Abaqus is used for the simulation purpose which provides ample information regarding total energy absorption of the crash box configurations before failure. Also the impact on the different crash box configurations provides the idea about its time to fail. Thus the crashworthiness deals with the energy absorption, crash box deformation and characteristics. The square, rectangular, hexagonal and pentagonal configurations are considered for the study. The configurations are simulated for the energy absorption study under impact load. During vehicle collision the crash box is supposed to absorb the impact energy which is its intended function. This research is carried out to design the configuration for crash box at conceptual design stage using Abaqus.**

Keywords: - Crash Box, Vehicle Safety, Crash Performance, Crashworthiness

I. INTRODUCTION

Crash boxes are generally made of steel with various compositions. A study is required for understanding the crash box behavior under impact. In addition, weight should be reduced while improving the performance. Crash box is a separate component in vehicle which is mounted in between main frame of the car and front bumper. At the time of the accident it deforms axially and absorbs accidental energy. Crash box structure provides comfort to the passenger at the time of impact. It works as safe guard for the costly components behind the bumper like engine hood and cooling system.

Nowadays thin walled structures have become very popular as energy absorbers because of their desirable energy absorption capacity, light weight and low cost. They are widely used in automobile, aerospace, defense and other industries. In the automobile design it has become very important to reduce the occurrence and consequences of accidents and to take effective precautions to minimize the damage.

In frontal collisions, the body structure performs different functions. The front is designed to act as a crumple zone, managing and absorbing crash energy by collapsing in a controlled manner, so that the impact affects the car and not the occupants. Crashworthiness is a measure of the vehicle's structural ability to plastically deform and yet maintain a sufficient survival space for its occupants in survivable crashes. Cars demonstrate maximum vehicle driving performance resulting from high tech developments in the area of lightweight materials and aerodynamic design. Since extreme racing speeds may lead to severe accidents with high amounts of energy involved, special measures were taken over a period of time in order to ensure the drivers safety in case of high-speed crashes. Besides the driver's protective equipment like helmet, harness or head and neck support device and the circuit's safety features like run-off areas and barriers, the car itself is designed for crashworthiness and possesses special sacrificial impact structures that absorb the race car's kinetic energy and limit the deceleration acting on the human body. At the moment every manufacturer has a different method of producing their crash structures. The choice of the material to

use is increasingly often dictated by weight and aerodynamic needs as well as structural performance. Recently it became preferable to make such structures in thin sheet material or composite materials, due to their advantages such as high strength to weight ratio, the high level of energy absorption and the possibility to reproduce complex geometry. The excellent performance of composites, sometimes better than those of similar metallic structures, can be obtained by choosing appropriate mechanical and geometrical design parameters.

The main objective of the study is to study the crashworthiness of the crash box and to find the energy absorbed by the different configurations of the crash box through Abaqus simulation software.

II. LITERATURE REVIEW

Yoshiaki Nakazawa et al. [1] studied and designed different cross sectional crash box so as to make sure it absorbs maximum energy. Li Qing-fen et al. [2] studied energy absorption characters and shape optimization design for thin walled tubes. He chose proper cross section and adopted appropriate grooves. He incorporated grooves at different location of six different crash boxes. Also used finite element analysis. Gangadhar Biradar [3] Used catia, hypermesh and L S dyna for modelling, meshing and simulating rectangular cross section crash box. Siva Kumar et al. [4] designed a crush box for different segment cars and checking its performance through numerical simulation. N Nasir Hussain et al. [5] comparing the different designs developed ne improved cross section conventional design and designed honey comb structure. Dhananjay D. Desai et al. [6] used analytical and experimental method to study plane crash box. M S I ShaikDawood et al. [7] used E-Glass/Epoxy material by developing grooved crash box. B A Constantine al [8] concentrated on the modern bumper which has to fulfil with the low speed urban impact, the load structure, the suitable regulation, the challenging needs of a modern front assembly and the finite element simulation of test is carried out. Gabriel Jiga et al. [9] identified that a light accident between automobiles, the interior of the car is damaged. Yanjie LIU et al. [10] applied the Finite Element (FE) method to model the structure and material of the crash-box. Modeling and simulation using the software LS-DYNA was carried out. Se-Jung Lee et al. [11] proposed study with multistep approach as one is a parameter study using discrete design with an orthogonal array.Man Yang [12] By coupling the design of styling and crash box's crash performance he designed a new technique in styling design phase and B-class car. B.P. DiPaolo et al. [13] performed an experimental investigation to study a specific axial crush configuration response of steel, square box components under quasi-static testing conditions. Kartik Solabannawar et al [14] improved the crashworthiness of the vehicle for front impact analysis by replacing the spot welds in the BIW structure with TOX joints.

A .Research Gap

Many of the researchers had studied the crash box as vehicle safety device using various methods like analysis, optimization, CAD, CAE, Simulation etc. Also different conventional materials are considered for the study. But still the problem of vehicle safety exists. Continuous improvement in case of crash box as safety device was carried out. But still none of the researcher have undergone with different cross sectional configurations of the crash box plate to increase the crash performance of the vehicle.

[1] Designs of honeycomb structure are comparatively very complicated

[2] Implementation of such structures requires highly advanced machinery

[3] Manufacturing of perfect grooves on such a small square cross sectional tubes is very difficult and cost involved is higher

[4] Honeycomb structure requires highly advanced machinery and skilled operator to used them causing greater cost involved for its manufacturing

[5] Some of the researchers analyzed the crash box designs with stress analysis and different CAD/CAM tools but actual simulation of for the deflection is not studied by them.

B. Problem Definition

While dealing with the impact the vehicles undergo major / minor damage or driver's safety might be hampered. Crash box is a safety structure which deals with this problem. The various structural combinations or shape along with materials may provide the best results which will substantially enhance the crash performance. A new or refined quantification methodology for improving crash performance of vehicle safety using crash box, based on computational, experimental and hybrid analyses is necessary for accurate evaluation prior to its implementation

III. METHODOLOGY

The paper discuss about the steps to be followed to achieve the objective of designing the crash box. This study and its execution will provide path for perfect implementation of steps with greater efficiency. There is no best way for material evaluation and selection therefore decision making applies variety of approaches. Material selection and evaluation is one of the key activities for design and metallurgy department in any organization, because it brings considerable savings as well as reduce risk hazards in company. Fig.1 describes the process of material selection for decision making.

Fig. 1.Decision Making Processes

A .Simulation Of Crash Box

The various configurations of the crash box may be arises from different combination but the simple and effective solution is the current need of the industry. The cross section of the product must be efficient to sustain at desired loads and impacts ensuring the vehicle and passenger safety. The following are the possible design configurations considered for the study as per the company's guidelines.

Abaqus is a set of influential engineering simulation curriculums built on the finite element method, sold by Dassault Systems as part of their SIMULIA Product Life-cycle Management(PLM).

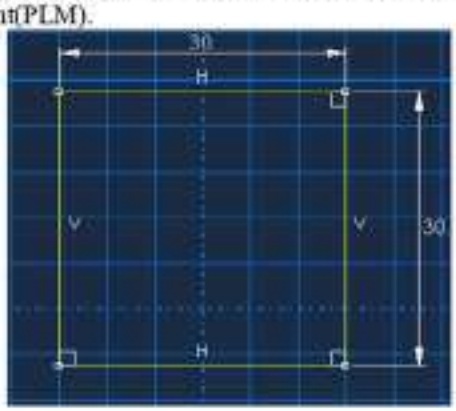

Fig.2. Square Configuration

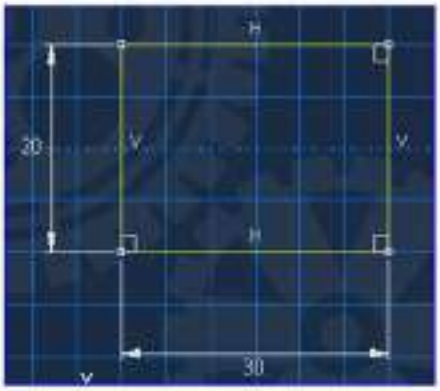

Fig.3. Rectangular Configuration

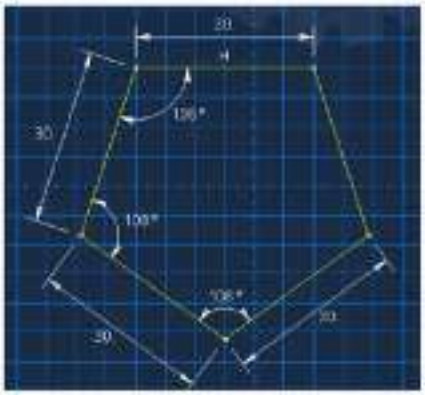

Fig.4. Pentagonal Configuration

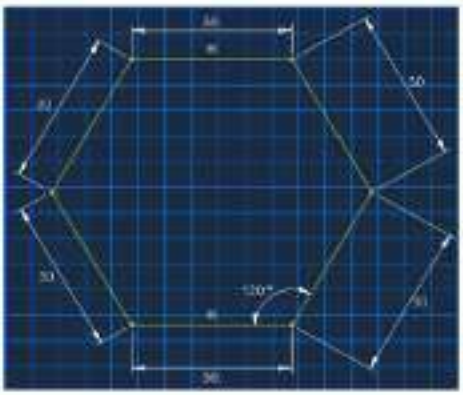

Fig.5. Hexagonal Configuration

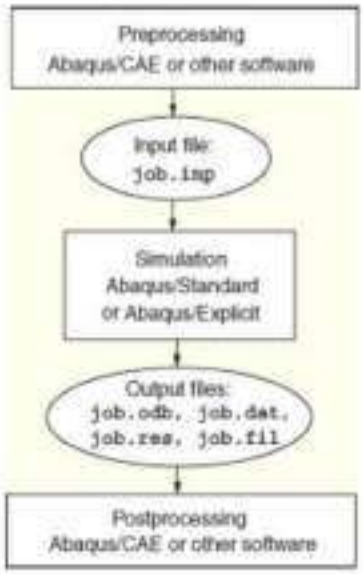

Fig.6 . Steps of Execution in abaqus

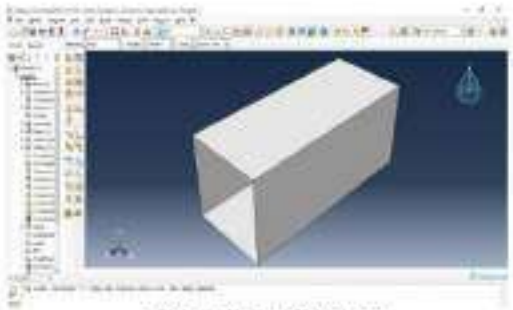

Fig.7. Model Creation

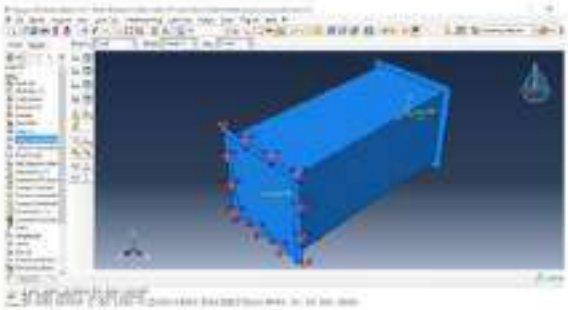

Fig.8. Boundary Conditions

Fig.9. Meshing

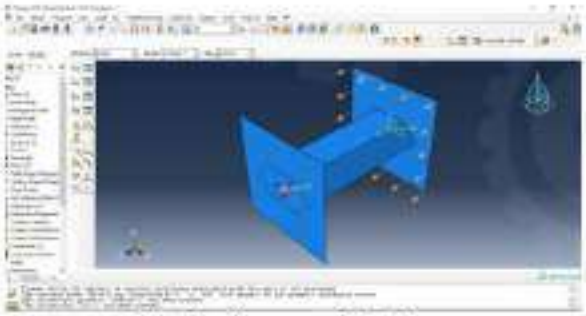

Fig.10. Hexagonal Model

IV. RESULTS

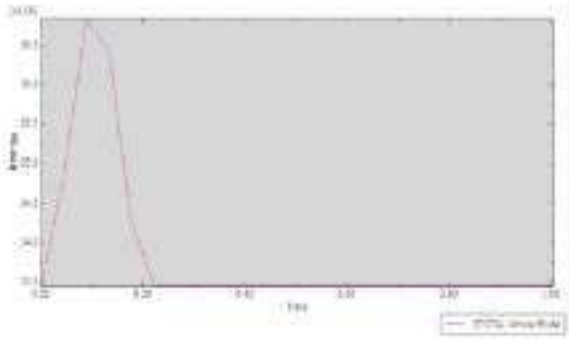

Fig.12. Total Energy Absorbed by Square Tube

The total energy absorbed by the square configuration of crash box is 36.5 X10^6 J and it crashes in 0.20 sec.

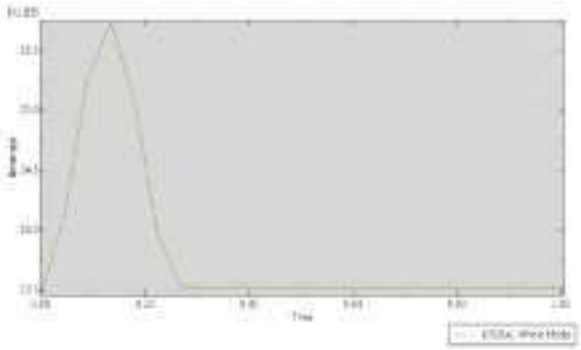

Fig.13. Total Energy Absorbed in Rectangular Tube

The total energy absorbed by the rectangular configuration of crash box is 35.5 X10^6 J and it crashes in 0.28 sec.

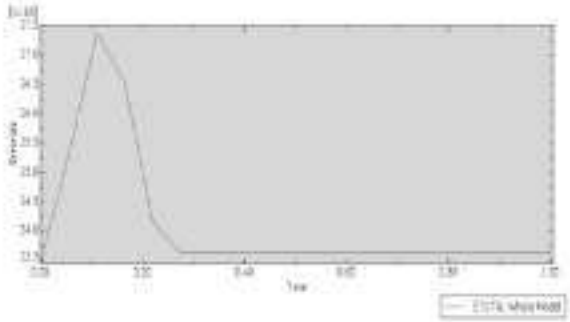

Fig.14. Total Energy Absorbed by Hexagonal Tube

The total energy absorbed by the hexagonal configuration of crash box is 37X10^6 J and it crashes in 0.28 sec.

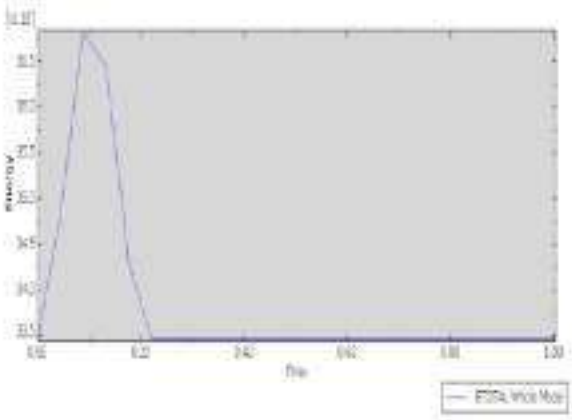

Fig.15. Energy Absorbed by Pentagonal Configuration

The total energy absorbed by the pentagonal configuration of crash box is 36.5X10^6 J and it crashes in 0.20 sec.

The above graphs of the energy absorbed depicts that the energy absorbed by the hexagonal cross section of the crash box absorbs more energy as compare to the remaining crash box configurations and takes slightly greater time to crash than other configurations. Hexagonal crash box configuration gives better results for the frontal collisions incidents than other compared configurations of the crash box.

V. EXPERIMENTATION

The different manufactured samples are tested on the Low velocity impact test machine for finding out the total absorbed energy by the individual sample manufactured.

The experimentation for the square, rectangular, pentagonal, hexagonal configurations is carried out to find the energy absorbed by these crash boxes. The low velocity impact tester machine is used for the purpose. After clamping the specimen in the fixture, the top head was put down to see if it rested on the top surface of the specimen correctly. The low velocity impact testing is taken to find the max energy absorbed by the crash box configurations prior to failure.

Fig.17. Low Velocity Impact Tester

VI. CONCLUSION

The energy absorbed by the different design configurations for automobile crash box are analyzed with the help of Abaqus and experiment. Crash box components absorbing energy are studied through basic types of different cross sections. Square and Rectangular profile have significant lower energy absorption than the other profiles. Hexagonal configuration absorbs more energy than the other configuration and sustains comparatively for more time than other configurations.

REFERENCES

[1] Yoshiaki Nakazawa, Kenji Tamura, Michitaka Yoshida, Katsutoshi Takagi, Mitsutoshi Kino, "Development Of Crash-Box For Passenger Car With High Capability For Energy Absorption", VIII International Conference on Computational Plasticity, 2005

[2] Li Qing-fen, "Finite Element Analysis and Shape Optimization of Automotive Crash-box Subjected to Low Velocity Impact", International Conference on Measuring Technology and Mechatronics Automation, 2009

[3] GangadharBiradar, AnjanBabu V.A, "Automotive Crash Box Performance Analysis and Simulation during Frontal Rigid Barrier Crash", International Journal of Science and Research, ISSN: 2319-7064, 2012

[4] A. Siva Kumar, G.Hunabindu, M.Sankar Raman, K. Vijaya Kumar Reddy, " Experimental Investigations with Crush Box Simulations for Different Segment Cars using LS-DYNA, International Journal of Current Engineering and Technology, E-ISSN 2277 – 4106, P-ISSN 2347 – 5161, 2014

[5] N NasirHussain, "Automobile Crash Box Design Improvement Using HyperStudy", Altair Technology Conference, 2015

[6] Dhananjay D. Desai, M. A. Kadam, "Analysis and Development of Energy Absorbing Crash Box", International journal of Advance Research and Innovative Ideas in Education, ISSN (O)-2395-4396, 2016

[7] M S I ShaikDawood, A L Ahmad Ghazilan, Q H Shah, "Finite element analysis of a composite crash box subjected to low velocity impact", International Conference on Mechanical, Automotive and Aerospace Engineering 2016.

[8] B A Constantin, "Studies about the Behavior of the Crash Boxes of a Car Body", International Engineering Research and Innovation Symposium, Materials Science and Engineering, 2016

[9] Gabriel Jiga, ŞtefanStanin, Gabriela Dinu, Daniel Vlăsceanu, DorinaPopovici, "Material and shape crash-box influence on the evaluation of the impact energy absorption capacity during a vehicle collision", Ciência&Tecnologia dos Materiais 28, 2016K. Elissa, "Title of paper if known," unpublished.

[10] Yanjie LIU, Lin DING, "A Study of using Different Crash Box Types in Automobile Frontal Collision", IJSSST, ISSN: 1473-804x online, 1473-8031

[11] Se-Jung Lee, Hyun-Ah Lee, Sang-Il Yi, Dae-Seung Kim, Heui Won Yang and Gyung-Jin Park, "Design flow for the crash box in a vehicle to maximize energy absorption", Proceedings of the Institution of Mechanical Engineers, Part D: Journal of Automobile Engineering, 2012

[12] Man Yang, "The Design of Car's Crash Box Based on the Section Force", Springer Publication, Proceedings of the FISITA 2012 World Automotive Congress, 2012

[13] B.P. DiPaolo, J.G. Tom, "A study on an axial crush configuration response of thin-wall, steel box components: The quasi-static experiments", International Journal of Solids and Structures, 2006

[14] Kartik Solabannavar, S. I. Bekinal, "To Simulate and Study the Behavior of Vehicle Front Structure Through Tox Joints in Frontal Collisions", International Research Journal of Engineering and Technology, Volume: 03 Issue: 07, July-2016

APPLICATION OF THERMAL IMAGING CAMERA FOR FINDING THE RIPENING OF FRUIT

Krishnamohan S Menon*, Dr Priam Pillai**

*Pillai College of Engineering, Mumbai University
** Professor, Pillai College of Engineering, Mumbai University.
*mkrishna@mes.ac.in, **ppillai@mes.ac.in.

Abstract:

75% of food consumed in India is produced in our own country. The farmers are directly affected by agriculture conditions. A lot of food produced goes waste as a result of improper & inadequate handling and storage condition and this directly affects the financial status of the farmer and consequently that of our own country too. Many a times a surplus in agriculture production with a potential for higher revenues goes waste due to lack of cold storage facility and improper transportation. Also many a times to protect the food supply the flow of food from farmers to consumers has many middle order agents such as the transporter, supplier, cold storage agents, retailers due to which the farmers get a very less percentage of the actual cost of the food. Also now-a-days people of cities go for organic fruits and vegetables and they choose for terrace farming and garden farming. In this scenario to get the maximum benefits from the agriculture products, it would be beneficial to farmers and also for the people of cities who choose for organic farming, if they had a system to identify and control the ripening of fruits and vegetables so that they can reduce the wastage of fruits and vegetables due to rotting and get maximum productivity and the value for their work. In this work a periodic monitoring of surface temperature of a fruit like apple has been done using a thermal camera and a continuous monitoring by LabVIEW using thermo-couple sensor. No particular co-relation was found between the surface temperature of the apple and the ripening rate.

Keywords:
Ripening, Thermal Imaging Camera, LabVIEW, Thermo-couple

I. INTRODUCTION

India is an agriculture based country. India has very poor rural roads, thus it affects the transportation of supply and output. Regional floods, lack of cold storage all spoils 30% of the surplus produced. Lack of organized retail limits Indian farmer's ability to sell the surplus and commercial crops. Indian farmers receive only 10-23% of price the consumer pays for the same produce due to inefficiencies & middle men. Farmers of developed countries such as Europe and US receive 64-81% [1].

Another reason found for the loss is that, every third food produced in agriculture, rots due to inefficient supply chain. The absence of factor to distinguish the three stages of maturity of fruit viz: immature, mature and over-ripe causes the fruit to rot as it isn't picked up at proper time. All these reasons lead to economic loss of our country and more concern as farmers incurs maximum loss for they give away their lives. Mature stage in maturity or ripen means that the fruit has gained the aesthetic characteristic which is seen by changes in concentration, colour, shades, smell, taste or other sensory properties [2]. Maturity evaluation is an important factor or step while harvesting and storing fruits [3]. In early ages, the fruit is considered to be ripening by visual impacts or sensory parameters such as its colour, smell, texture and taste. But in medieval ages due to artificial ripening and due to addition of chemicals or by giving a layer of wax over the fruit surface (e.g.: in case of apples), the fruit outer skin gets the colour that it gets when ripen though inside the flesh is still immature. It also harms human health. Therefore there is a need of an optimized and cheaper technique of storing the matured fruits and

identify the maturity of fruits by other way than visual parameters. There is also a need to find a condition that will help in controlling the rate of ripening of fruits in natural way. As ripening is a biological change there must be a heat output or heat input that is exothermic or endothermic reaction and thus there must be a relation with its surface temperature as temperature affects most of the biological processes in the development of fruits which in turn influences fruit-size, colour, sugar content, acid content, starch content, smell, etc [4].

IR thermo-graphy is an example of infrared imaging science that detects IR range of bands in the electromagnetic spectrum. Every substance surfaces emits infrared radiation with relation to the temperature of the surface of the substance [9].

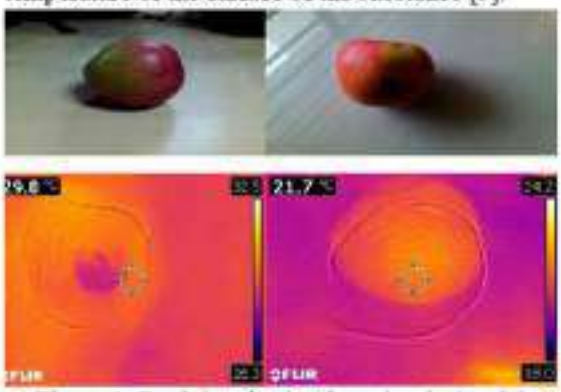

Figure 1: Real time bruise detection in (apple) fruits using thermal camera [5]

Figure 1 shows the image of an apple that was taken by normal camera and Infrared camera for detection of bruise in apples [5]. Thus Thermal imaging camera helps to get thermal images of fruit surface and the variation of the temperature could be known by the different spectrum band and the temperature value also could be measured.

II. Methodology

The fruit that chosen must be an all season fruit so that the availability doesn't affect and fresh fruits are available during experiment or research work. The variation of temperature with ripening will be monitored continuously to determine the optimized temperature and ambient condition (temperature) at which they will be ripened fast. Periodic monitoring will be done by thermal imaging camera and continuous monitoring by LabVIEW software. The relation between the surface temperature and ripening will be studied with the help of the graph. With this result a simple and cheap storing system will be designed and fabricated. This will help to discuss the optimized temperature at which fruit ripening can be controlled.

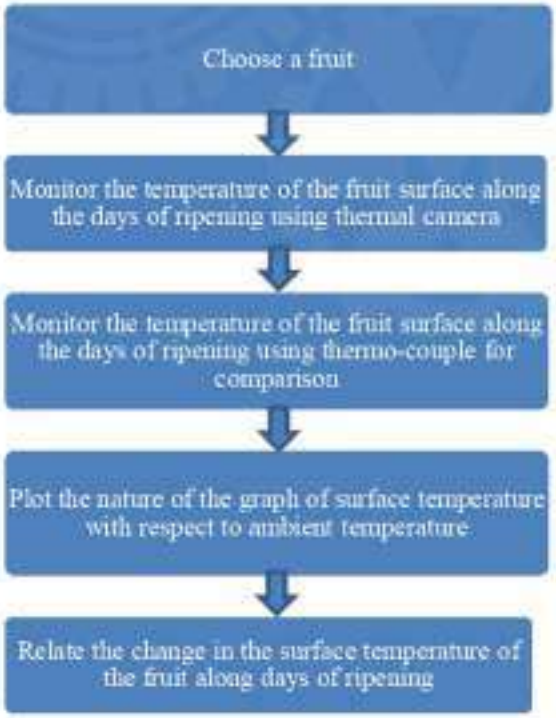

Fig 2: Process Flow

III. Experimentation

A. Monitoring of fruit using Thermal Camera

The fruit surface temperature was monitored and recorded using Thermal Imaging Camera and along with the picture was taken by ordinary camera. Following set of readings were taken through the days of incubation by thermal camera.

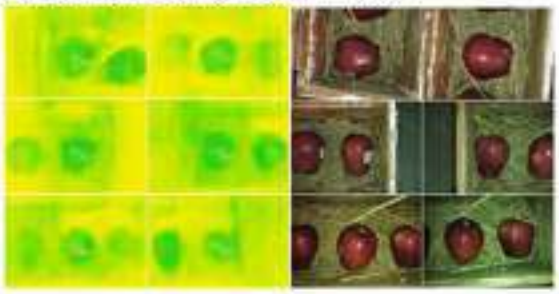

Figure 3: Comparison between the actual images and thermal camera images for day 1

The above readings and images show the results for the thermal camera picture and normal camera picture for Day 1 of 6 different apples.

identify the maturity of fruits by other way than visual parameters. There is also a need to find a condition that will help in controlling the rate of ripening of fruits in natural way. As ripening is a biological change there must be a heat output or heat input that is exothermic or endothermic reaction and thus there must be a relation with its surface temperature as temperature affects most of the biological processes in the development of fruits which in turn influences fruit-size, colour, sugar content, acid content, starch content, smell, etc [4].

IR thermo-graphy is an example of infrared imaging science that detects IR range of bands in the electromagnetic spectrum. Every substance surfaces emits infrared radiation with relation to the temperature of the surface of the substance [9].

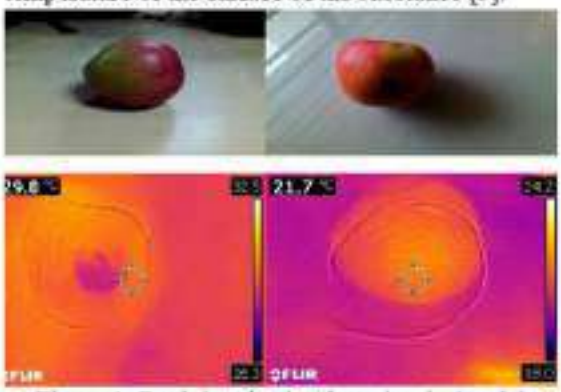

Figure 1: Real time bruise detection in (apple) fruits using thermal camera [5]

Figure 1 shows the image of an apple that was taken by normal camera and Infrared camera for detection of bruise in apples [5]. Thus Thermal imaging camera helps to get thermal images of fruit surface and the variation of the temperature could be known by the different spectrum band and the temperature value also could be measured.

II. Methodology

The fruit that chosen must be an all season fruit so that the availability doesn't affect and fresh fruits are available during experiment or research work. The variation of temperature with ripening will be monitored continuously to determine the optimized temperature and ambient condition (temperature) at which they will be ripened fast. Periodic monitoring will be done by thermal imaging camera and continuous monitoring by LabVIEW software. The relation between the surface temperature and ripening will be studied with the help of the graph. With this result a simple and cheap storing system will be designed and fabricated. This will help to discuss the optimized temperature at which fruit ripening can be controlled.

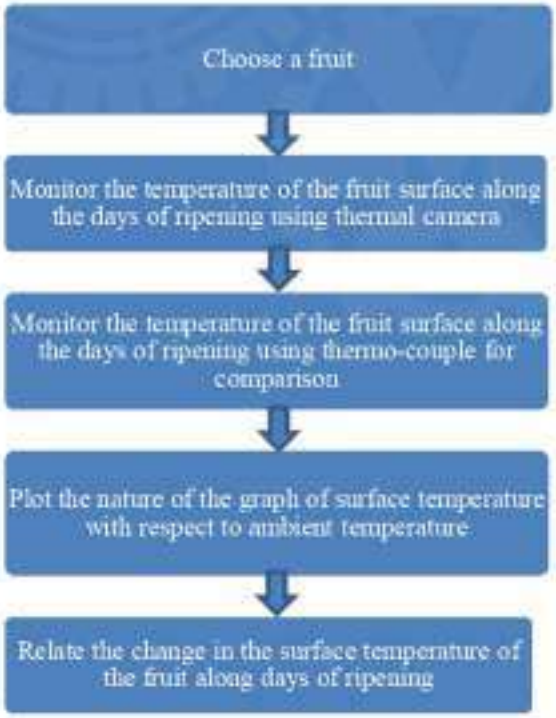

Fig 2: Process Flow

III. Experimentation

A. Monitoring of fruit using Thermal Camera

The fruit surface temperature was monitored and recorded using Thermal Imaging Camera and along with the picture was taken by ordinary camera. Following set of readings were taken through the days of incubation by thermal camera.

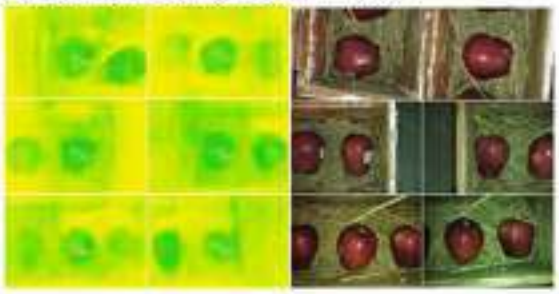

Figure 3: Comparison between the actual images and thermal camera images for day 1

The above readings and images show the results for the thermal camera picture and normal camera picture for Day 1 of 6 different apples.

Figure 4: Comparison between the actual images and thermal camera images for day 2

The above readings and images show the results for the thermal camera picture and normal camera picture for Day 2 of 6 apples that was kept on Day 1.

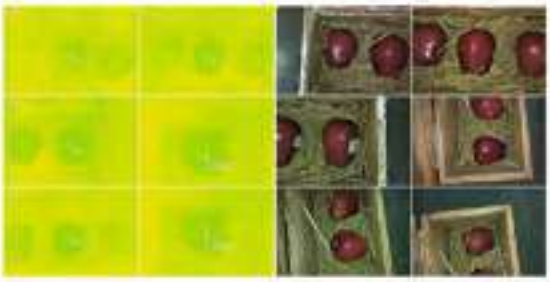

Figure 5: Comparison between the actual images and thermal camera images for day 3

The above readings and images show the results for the thermal camera picture and normal camera picture for Day 3 of 6 apples that was kept on Day 1.

Figure 6: Comparison between the actual images and thermal camera images for day 4

The above readings and images show the results for the thermal camera picture and normal camera picture for Day 4 of 6 apples that was kept on Day 1.

Figure 7: Comparison between the actual images and thermal camera images for day 5

The above readings and images show the results for the thermal camera picture and normal camera picture for Day 5 of 6 apples that was kept on Day 1. There is no much change in the temperature and the temperature shown in approximation. The above results show that there is no much change in the temperature with respect to the time and ripening stages. The colour pattern does not change with the days of ripening. It adapts the temperature of the surrounding and thus the colour pattern is uniform. The reason might be because of the poor resolution of the thermal camera. Another reason may be because of no temperature control system. In order to check whether the problem is because of the thermal camera or other cause the monitoring of the fruit was done using Lab VIEW.

B. Monitoring of fruit using LabVIEW

The thermo-couples were calibrated at first at 0^0C and 100^0C. Two thermo-couples sense temperatures of two apples named as Apple 1 and Apple 2. A thermal insulation tape was stuck in between the sticking tape and thermo-couple junction in order to avoid any heat generation due to sticking tape. The images below show how the junction is stuck to the surface of Apples.

Figure 8: Apple 1 and Apple 2 with TC

One thermo-couple was put freely inside the box near the surface of the apple to sense the inside temperature of the box, that is the inner ambient temperature. Then the box is filled with hay so as to maintain heat in equilibrium. The two images below shows the inner ambient temperature sensor thermo-couple and the box filled with hay.

Figure 9: TC for inner ambient and Box covered with Hay

One thermo-couple is attached to outer wall of the box for sensing the outer temperature. The box drilled hole is sealed from where thermo-couple 1, 2 and 3 were taken inside the box.

Figure 10: TC for outer ambient and gap sealed & box sealed

The thermo-couple senses temperature and these data are acquired by the Data Acquisition System the hardware for the lab view. These analog signals of temperature are converted into voltage signals by NI 9211 card (module), a module for the thermo-couple.

Figure 11: Setup and DAQ

Figure 12: Complete set-up

The data (temperature data) was acquired by Lab view. The circuits were made in lab view by building NI that is assisting data to acquire analog temperature signals. The readings were recorded after every 30 minutes.

IV. Results and Discussion

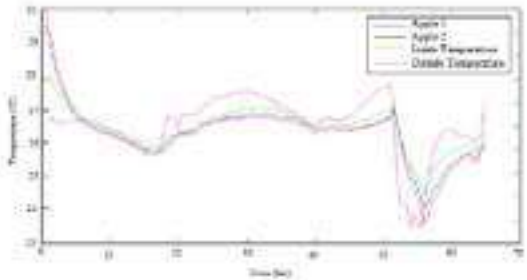

Figure 13: Graph showing the variation of temperatures with respect of time

The above graph was plotted for temperature reading for every 30 minutes for period of 4 days. From the above graph it is seen that at starting when the fruit were kept in the box the surface temperature of the apples is more compared to the ambient temperature of the inside and outside box. As time passed by the surface temperature of the fruit started falling down below the inside and outside surface temperature of the incubation box. Soon it was seen that the nature of the graph of the temperature of the surface of the apples and the inner ambient temperature of the box followed the outer ambient temperature curve. Thus no particular conclusion could be drawn from the first reading other than the conclusion that the temperature of the apple surface temperature decreases while ripening as mentioned in the literature.

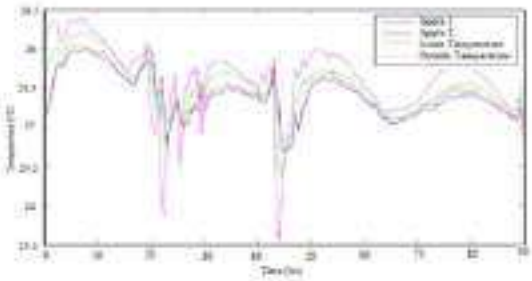

Figure 14: Graph showing the variation of temperatures with respect of time

The above graph was plotted for temperature reading for every 30 minutes for a period of 4 days. This time the initial surface temperature of the apples taken were kept less than the outer and inner ambient temperature of the box at the beginning. As time passed by the temperature of the surface of the apples were falling below the inner and outer ambient temperature of the box, showing that the surface of the apple temperatures remained less than the inner ambient temperature of the box followed after outer ambient temperature. Again it was seen that the nature of the graph of the temperature of the surface of the apples and the inner ambient temperature of the box follows or traces the outer ambient temperature path or curve. The temperature of the apple surface temperature again seems to decrease while ripening. The other thing that was noticed was the drop of temperature in equal interval of time. The reason might be sudden voltage drop or fluctuation as the drop was seen during the night hours in the graph.

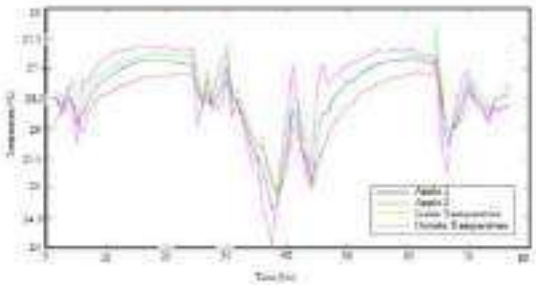

Figure 15: Graph showing the variation of temperatures with respect of time

The above graph was plotted for temperature reading for every 30 minutes for a period of 3 days. This time the initial surface temperature of the apples taken were kept less than the inner ambient temperature and more than the outer ambient temperature of the box at the beginning. Again the final temperatures of the apple surfaces and the curve of their temperature fell below the inner and outer ambient temperatures of the box. It was seen that the nature of the graph of the temperature of the surface of the apples and the inner ambient temperature of the box follows or traces the outer ambient temperature path or curve even in this set of reading. The temperature of the apple surface temperature again seems to decrease while ripening. There is again sudden drop of temperature in equal interval of time.

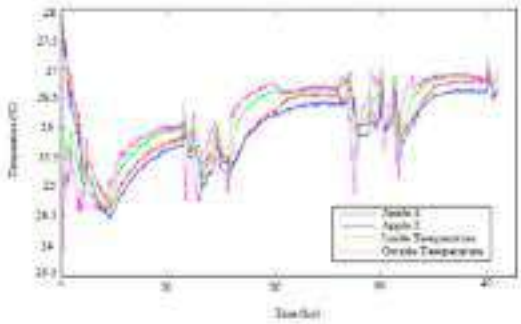

Figure 16: Graph showing the variation of temperatures with respect of time

The above graph was plotted for temperature reading for every 30 minutes with box insulated using thermocol for a period of 2 days. At starting when the fruit were kept in the box the surface temperature of the apples is more compared to the ambient temperature of the inside and outside box. As time passed by the surface temperature of the fruit started falling down below the inside and outside surface temperature of the incubation box. Soon it was seen that the nature of the graph of the temperature of the surface of the apples and the inner ambient temperature of the box followed the outer ambient temperature curve. The temperature of the apple surface temperature was seen decreasing while ripening. As the readings in the graph tells us that the inner surface temperature just replicates the nature of graph of outer ambient condition it was difficult to come in any conclusion where the surface temperature of the fruit can be monitored through the period of ripening.

V. Conclusions

The results from the thermal camera images show that there is not much change in the temperature though it should rise while ripening as per the referred literature. The reason might be because of the camera quality and measurement precision. The thermal camera which was used for the experimentation was of very low pixel/resolution and specification. It had the issue of range as it was inaccurate working in range more than 1 meter,

which is the thermal camera would show very inaccurate reading if the distance of the object and the thermal camera is more than 1 meter. Also the thermal camera used did not show proper thermal gradient by the different colour patterns of temperature and the temperature readings was also less approximate. These reasons made it difficult to monitor the actual temperature variation of a fruit along with time during the stages of ripening.

The results of temperature graph and variance of Lab VIEW shows that the surface temperature of the fruit traces the path of the outer ambient temperature throughout the day. Thus, it is concluded that the results do not show a particular characteristic which can help us to focus on the ripening temperature.

REFERENCES

1. P K Kingra, Debjyoti Majumder, Som Pal Singh, "Application of Remote Sensing & GIS in agriculture and natural resource management under changing climatic conditions", *Agriculture Research Journal, Volume 53, Issue 3*, pp. 295-302, September, 2016.
2. A. A. Kader "Fruit maturity, Ripening, and Quality Relationships", *International Symposium on Effect of Pre-harvest and Post-harvest Factors on Storage of Fruit, Acta Horticulture* 485, pp. 203-208, ISHS 1999.
3. Annamalai Manickavasagan, Digvir S Jayas, Noel D G White, Jitendra Paliwal, "Application of thermal imaging in Agriculture – A Review", *Canadian Society for engineering in agricultural, food and biological systems*, pp. 05-002, June 26-29, 2005.
4. Lei Li et al, Troy Peters, Qin Zhang, Jingjin Zhang, Danfeng Huang, "Modeling Apple Surface Temperature Dynamics Based on Weather Data", *Sensors (Basel), Volume 14*, pp. 20217-20234, November 2014.
5. Manisha Satone , Samruddhi Divakar, Vaishnavi Joshi, "Automatic Bruise Detection in Fruits Using Thermal Images", *International Journal of Advanced Research in Computer Science and Software Engineering, Volume 7, Issue 5*, pp. 727 – 732, May, 2017.
6. Prof. S. N. Naik, "Ripening- an important process in fruit development" in SCRIBD uploaded by Wed D Gorden, Retrieved from www.scribd.com/doc/170345242/fruit-ripening-by-Prof-S-N-Naik-IIT-Delhi last visited: 20/08/2017
7. D. C. Slaughter, J. A. Abbott, "Applications in analysis of fruits and vegetables", *Near-Infrared Spectroscopy in Agriculture Agronomy Monograph*, no. 44, pp. 1-12, 2004.
8. Md. Anowar Hossain, Md. Masud Rana, Yoshinobu Kimura, Hairul Azman Roslan, "Changes in Biochemical Characteristics and Activities of ripening associated enzymes in Mango fruit during the storage at different temperatures", *Biomed Research International, Vol 2014*, Article ID 232969, July 2014.
9. Poryev, V. A., Poryev, G. V. (2004). "Experimental determination of the temperature range of a television pyrometer" *Journal of Optical Technology, Volume 71 (1)*, pp. 70–71, 2004.
10. Samira Ben Mussa, Intisar El Sharaa, "Analysis of Vitamin C (ascorbic acid) Contents packed fruit juice by UV spectrophotometry and Redox Titration Method", *IOSR Journal of Applied Physics (IOSR-Jap) e-ISSN: 2278-4861.Volume 6, Issue 5* Ver. II (Sep.-Oct. 2014)
11. Jeffrey, Travise, "LabVIEW for everyone Graphical programming made easy and fun", *King Jin*, 3rd edition, Upper Seddle River, NJ: Prentice Hall, 2006.
12. (2014). "National Instrument Datasheet", retrieved from: www.ni.com/pdf/manuals/3734669_02.pdf last visited: 04/01/16
13. EditorX, "Thermocouple", in Temperatures.com, Feb 27, 2009. Retrieved from: https://www.temperatures.com/sensors/csensors/thermocouples-tcs/ last visited: March, 2016.
14. (2015). "National Instruments". Retrieved from http://www.ni.com/en-in/shop/labview.html last visited: Feb 2016
15. (2014). "Flir One Thermal Camera". Retrieved from https://www.pcmag.com/article2/0,2817,2462176,00.asp
Last visited: Jan, 2016

MAGNETIC-ACTUATOR USING FERROFLUID-POLYMER COMPOSITE

Shridhar S Deshmukh,

Advised *by* Dr. *Priam V Pillai*, Ph.D.

Department of Mechanical Engineering, Pillai Institute of Information Technology,
New Panvel, Raigad, India.
Email. Shridhardeshmukh1001@gmail.com,
ppillai@mes.ac.in.

***Abstract*—In this paper we have developed a silicone rubber-ferrofluid composite cantilever at micro-scale. The method of manufacturing is low cost using laser cutter to create a mould. The moulds are manufactured with methyl methacrylate sheet with 6 to 10 mm thickness. We are able to create cantilever that are randomly oriented or have a unidirectional distribution of magnetite particles or have magnetic particles at tip .Cantilever with 400 µm diameter and up to 10 mm length are tested with low magnetic field of 15 mT. We got maximum deflection of 82.5^0 at 44 mT magnetic field.**

***Keywords*—mPDMS; ferrofluid; cilia; cantilever**

I. Introduction

The undeveloped and new emerging field of smart materials triggers researchers mind to mimic the natural occurring structures. The nature has developed its system through optimization criteria like to allow small biological cells to do very complex task together. The analysis of such system at microscopic level gives us lots of new idea that can be used in engineering design to solve our problems. The two different materials are combined to form new composite, which gives enhanced properties than base materials. The smart materials are combined to form such composite called smart composite responsive to external stimuli. The nanosize magnetite (Fe_3O_4) particles can be entrapped in to elastomer by cross-linking reaction to form magnetic responsive elastic structure [4]. These magnetic particles has also been impregnated in porous materials like tissue paper to make magnetic responsive actuators [2], with these ferroelastic composite we get combined magnetic and elastic properties. These polymers composite gives good application as artificial cilia. Cilia and flagella are mainly used for movement exhibited by cells and sperms. Cilia are hair like structure responsible for much biological function like movement, taking in food particle [3].

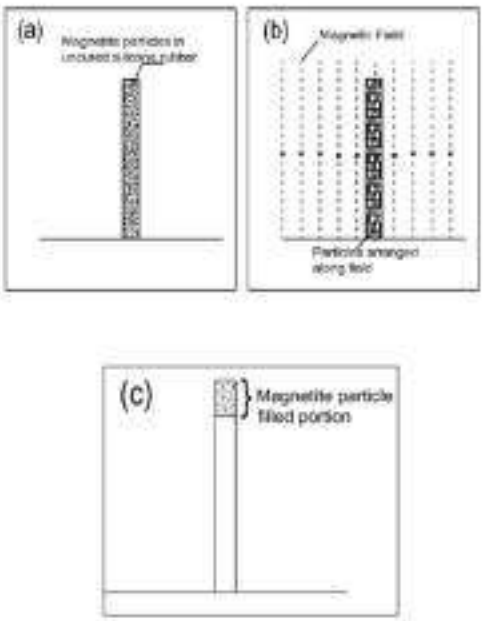

Fig. 1. Schematic of (a) Isotropic, (b) Anisotropic and (c) Tip composite cantilever samples (not to scale)

II. THEORY

The magnetic polymer contain magnetite particles dispersed in polymer network. These particle are connected to polymer chain by adhesive forces.In ferrofluid these nano size particle tends to agglomerate due to magnetic dipole interaction,this problem is solved by coating the particle with surfactant made of long chained molecule.[5].These particles in magnetic polymer are randomly oriented. As we apply external magnetic field the particle as dipole tends to align with field and produce magnetization, M [1].

$$M = < M.H > \div H = Ms < \cos \Theta > \qquad (1)$$

Where Θ is the angle between the magnetic axes of a particle, Ms is magnetic saturation H is the external field strength. The

average cosΘ is taken overall the particles. The silicon rubber gives economical elastic material to hold magnetite particle. These magnetic responsive polymer composite are known as mPDMS.

III. Result and Desscusion

The magnetic silicone rubber is prepared by various methods. One method is ferrofluid mixed with polymer and allowed polymer to cure and arrest magnetite particles in to polymer network. Another method is to coat polymer with magnetite particle using adhesive. Here we have prepared polymer by first method and different samples are tested at different magnetic field.

The silicone rubber is prepared by mixing commercially available (A-B silicone compound from SMOOTH-ON-OOMOO-30) polymer compound in ratio of 1:1 by volume. It is easy to use silicone rubber compounds that feature convenient one-to-one by volume mix ratios (no scale necessary). Both have very low viscosity for easy mixing and pouring and vacuum degassing is usually not necessary. This product cures at room temperature with negligible shrinkage and have good tear strength.

The ferrofluid is mixed with uncured silicone rubber (20 % by volume of polymer).Polymer mixture with ferrofluid is poured in moulds for 7 hr at temp 23^0 C for complete curing of polymer composite. The amount of ferrofluid can be varied to change magnetic and mechanical properties of composite. The mould for casting the cantilever is manufactured in methyl methacrylate 10mm sheet. The cavity in sheet is made by laser engraver (LaserPro, spirit) with thickness of laser 0.001 inch.
Three samples of cantilever are compared :-
(I) Isotropic composite
(II)Anisotropic composite
(III) Tip loaded with magnetite particle.
The magnetite particles in composite are randomly distributed that composite shows Isotropic properties and called isotropic composite as shown in fig. 1. (a)
Second sample is prepared by keeping the mould in uniform magnetic field during curing process, Because of magnetic field the magnetite particle gets arranged along magnetic field direction. Fig.3. shows the microscopic image of composite prepared in absence of magnetic field and in presence of magnetic field. Mould is kept for 7 hr (curing period of polymer) in uniform magnetic field to fix the unidirectional arrangement of particles.

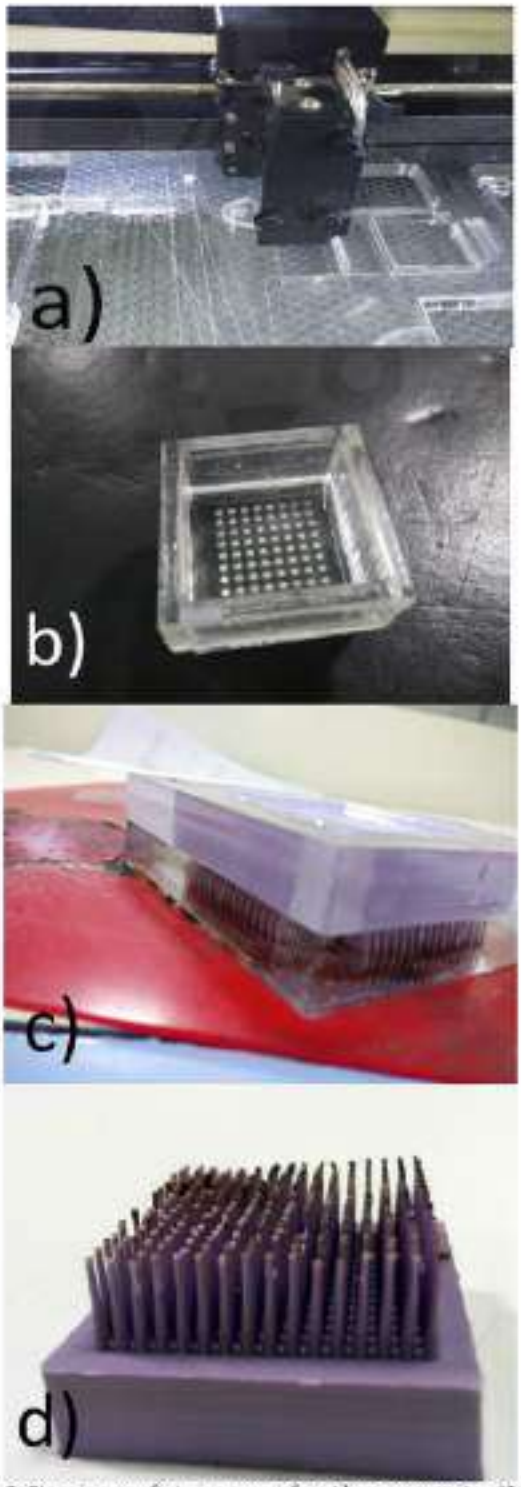

Fig. 2. Steps in manufacturing array of cantilever composite, a)Laser engraving process on acrylic sheet b)Finished acrylic mould with holes c)liquid silicon compound mixed with ferrofluid poured in mould d)Array of silicon ferrofluid composite after 6hrs

The particles are arranged along length of cantilever giving anisotropic properties, called anisotropic composite, the preparation of anisotropic composite is shown in fig.1.(b).Third sample is made having magnetic particles at the tip.fig. 2. (c) shows the cantilever body is made up of

silicone rubber and the tip band of 1 mm from free end is filled with magnetite particle.

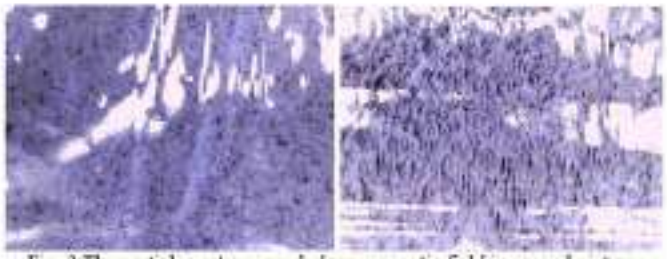

Fig. 3.The particles get arranged along magnetic field in second picture.

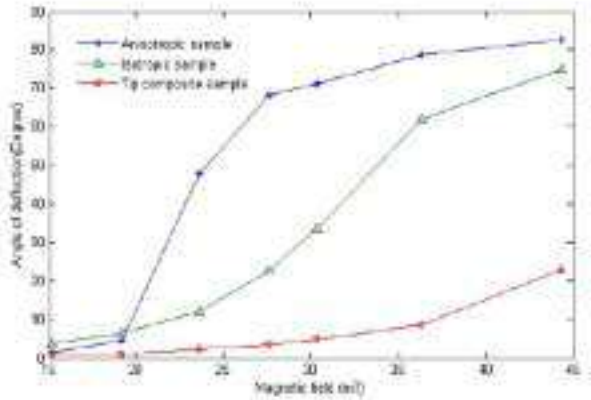

Fig. 4. Bending angle vs magnetic field Comparison of three samples. Dimension of cantilever (400 μm dia, 10 mm length)

A single cantilever of each sample is subjected to different magnetic field 0 mT to 44 mT to check its response. The neodymium magnets (K & J Magnetics, inc. Jamison) are used to create magnetic field. The magnetic field direction was perpendicular to length of cantilever. The magnetic field is measured with Hall probe at the tip of cantilever. Each sample of cantilever is kept in magnetic field and the image is acquired with microscope (Dino-Lite digital microscope AM3011).Deflection images from microscope are processed in MATLAB (Matlab R2013a). The RGB image is converted into grayscale and again to black_white to measure deflection angle. All the images are processed on matlab for angle measurement. Figure 4 shows the magnetic field vs angle of deflection. As can be seen the anisotropic sample shows more deflection compared to isotropic and tip composite cantilever. Anisotropic cantilever has particle fixed in polymer chain and oriented along length as shown in fig.3. When magnetic field perpendicular to length of cantilever is applied, these particles together try to orient along direction of applied magnetic field. As magnetite particles are fixed in polymer, the whole cantilever gets deflected giving larger angle. The field can be applied from opposite direction to reverse the deflection. Isotropic cantilever have well dispersed magnetite particles can be considered cantilever beam with uniformly distributed load through its length. In case of tip composite cantilever the magnetic field acts at its tip only , gives lower defection that isotropic and anisotropic cantilever.

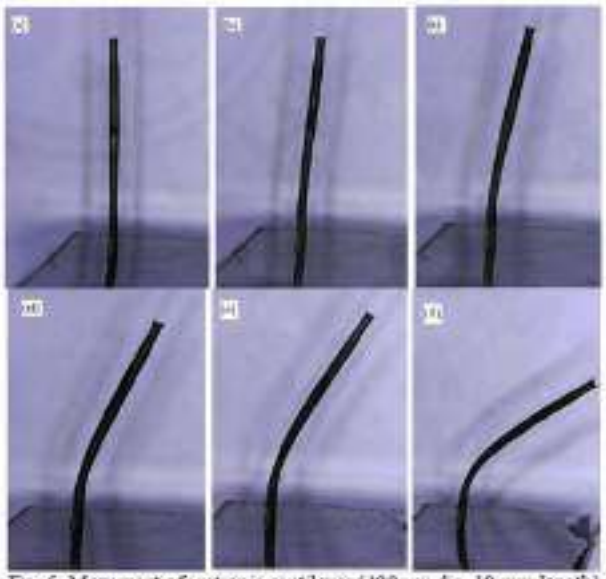

Fig. 5. Movement of isotropic cantilever (400 μm dia, 10 mm length) under magnetic field ranging (a) 0 mT to (f) 36 mT.

The fig.5 shows isotropic cantilever subjected to different magnetic field from 0 mT to 36 mT in one direction.

IV. CONCLUSION

We have fabricated magnetic responsive cantilevers. These cantilevers can be used as actuators. We reported cheap and simple method to manufacture these micro level cantilevers. These cantilevers were tested at different magnetic field. Three different samples were tested as anisotropic, isotropic and tip composite. The anisotropic sample showed better response (82^0deflection for several miliTesla) as compared to other iso and tip composite. Cantilevers from mm level to microlevels were manufactured using methyl methacrylate material moulds. Laser engraving gives cheap and effective method to manufacture these moulds. These cantilevers has optimum applications as artificial cilia, micro pump and micro Valves.

V. REFERENCES

[1] G.Filipcsei,I.Csetneki, A. Szilagyi, M. Zrinyi, "Magnetic field-responsive smart polymer composites," Springer-Verlag Berlin Heidelberg , pp. 137-189, jan 2007.

[2] Zhenwen Ding, Pinglning Wei, and Babak Ziaie, "Ferro-paper actuator," IEEE MEMS,Hong kong,pp. 1127-1130, Jan 2010.

[3] Ali Ghanbari, Mohsen Bahrami, "A novel swimming microrobot based on artificial cilia for biomedical applications,"Springer J Intell Robot Syst, vol. 63, Netherland, pp.399-416,Sept 2011.

[4] S. de Pedro, V. . J. Cadarso, X.Munoz-Berbel,J.A.Plaza, J.Sort,J.Brugger ,S. Buttgenbach,et al."Magnetically-actuated variable optical attenuators using ferrofluid-doped elastomer implemented by combination of soft lithography and inkjet printing technologies"IEEE MEMS, Taiwan,pp.548-551,Jan 2013.

[5] S.Odenbach,"Ferrofluids-magnetically controlled suspensions,"Elsevier, Colloids and Surfaces,vol 217,Germany,pp.171-178,2003.

Condensation Heat Transfer In Helical Coil

Tikaram G. Verma, B. Prof. Rashed Ali,

Department of mechanical engineering, Pillai college of engineering,University of Mumbai,

[A]Email:vtganpat@mes.ac.in, [B]Email:rashedali@mes.ac.in

Abstract— **The purpose of this research is to study the effect of the coil diameter and inlet temperature of steam on the heat transfer co-efficient and temperature drop in the helical coil. The study was based on fluid to fluid heat transfer. Experiments were conducted on two different mass flow rate of water. Inlet temperature of steam ranging from 100^0 C to 110^0 C are considered and various heat transfer coefficients are calculated for the above range. To serve the purpose experimental setup was built with three different helical coil and water tank. The result shows that there there is increase in heat transfer coefficient with increase in inlet temperature of steam.**

Keywords: Heat Transfer Co-efficient, Helical Coil, Mass Flow Rate

I. Introduction

Heat transfer is one of the most important physical processes. Different type of heat exchangers are designed and fabricated for different heat transfer applications. Heat exchangers are designed to get an efficient method of heat transfer from one fluid to other fluid. The three principles of heat transfer are: conduction, convection and radiation. In a heat exchanger the radiation heat transfer is not taken into account as it is negligible as compared to conduction and convection. There are different heat transfer enhancement techniques: Active, passive and compound. Application of electric, and magnetic fields and fluid /system vibration are active techniques. Helical coils, additives, rough and extended surfaces, swirl flow devices, are all passive enhancement techniques. Passive methods are preferred over active methods because of ease in manufacturing, low cost and longer life.

Curved tubes are widely used passive heat transfer enhancement technique in several heat transfer applications. Heat transfer enhancement by using helical coil has been researched and studied by many researchers. Various helical coil configurations are possible, and the most common configuration is of vertically stacked helically coiled tube. The end of the tubes act as the inlet and outlet for hot as well as cold fluid. This configuration offers compact structure and high heat transfer. Helical coils offer advantages over straight tubes due to their compact structure and higher heat transfer

Coefficients. Helically coiled heat exchangers are widely used in industrial applications such as power sector,food processing units, heat recovery systems, refrigeration and air conditioning, HVACs etc.

A. Heat transfer enhancement and secondary flow in coiled tubes

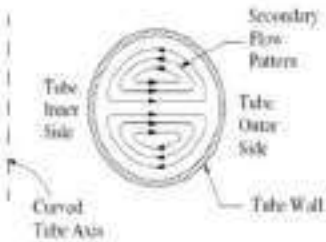

Fig. 1 Secondary flow in helical coil [1]

Due to the curved shape of the tube the flowing fluid inside the coil experiences centrifugal force. The centrifugal force depends on the velocity of the fluid particle and coil diameter. The velocity of fluid particles flowing at the center of the pipe is higher than the fluid particles flowing near to the pipe wall. Thus the centrifugal force on fluid particles flowing close to the tube wall is lower than the fluid particles flowing in the core. This difference in centrifugal forces causes the fluid from the core region to be pushed towards the outer wall of tube. The stream bifurcates at the wall and the fluid move towards the inner wall along the tube periphery, causing generation of secondary flows. This secondary flow produces additional convective transport of fluid which increases both the heat transfer and the pressure drop as compared to straight tube of same dimension.

Significant experimental research has been reported for single phase flow in helical coil and two phase flow in straight tubes. However, very limited heat transfer studies have been reported in the literature for two phase flow in helical coils.

Additionally, very limited number of studies reported on condensation heat transfer using steam in helical coils.

II. LITERATURE REVIEW

This chapter presents a review of the research done on heat transfer in helical coils. Several studies have indicated that helical coiled tubes are superior to straight tubes when employed in heat transfer applications. Secondly, a review of experimental work of condensation heat transfer in straight coils is presented. Next review of the research done on condensation heat transfer in helical coil.

Liung zhao (2003) et al studied the boiling heat transfer characteristics and pressure drop of steam-water two-phase flow in a small horizontal helically coiled tubing once-through steam generators. They have obtained a new two-phase frictional pressure drop co-relation. It was found that boiling heat transfer dependent on both mass flux and heat flux. Both the nucleation and the convection have the same importance to forced convective boiling heat transfer. The frictional pressure drop multiplier of two phase flow is a function not only of the mass quality and pressure, but also of the mass flow rate. [2]

Prabhajan (2004) performed an experiment study on natural convection heat transfer from helical coiled tubes in water. Experimental set up made up of 4 coils, 3 flow rates, and 2 water bath temperatures. In this study he correlated the outside Nusselt number to the Rayleigh number using different characteristic lengths it was found that the coil height is the best characteristic length for a vertical coil in this study. He further developed a prediction model to predict the outlet temperature of a fluid flowing through a helically coiled heat exchanger if the inlet temperature, bath temperature, coil dimensions, and fluid flow rate is known.

In his study he compared the predicted outlet temperature with the measured values from experimental setup. It was found that the results of the predicted temperatures were closer to the experimental values.[3]

M.H. Al-Hajeri (2007) et al experimental investigated the condensation heat transfer and pressure drop of an ozone friendly refrigerant, R-134a, inside a helical tube for climatic conditioning of hot regions. This study concerns the condensation of R-134a flowing through annular helical tubes with different operating refrigerant saturated temperatures. The average pressure drop is measured and compared with data from relevant literature. The measurements of R-134a were performed on mass flow flux ranges from 50 to 680 kg/m2 s. The study provides experimental data that could be used for the design and development of more efficient condensers for refrigeration and air conditioning (A/C) systems working with the same refrigerant. They have found that heat transfer coefficient and overall heat transfer coefficient of the refrigerant side decrease as the vapor saturated temperatures of R-134a increase. Pressure drops in annular helical tubes increase as the mass flux of refrigerant increase. [4]

Jayakumar (2008) fabricated an experimental setup to study fluid–fluid heat transfer in a helically coiled heat exchanger. Heat transfer characteristics of the helical coil heat exchanger are also studied using the CFD code FLUENT. The CFD predictions and the experimental results matched reasonably well within experimental error limits. Based on this results a correlation was developed to for inner heat transfer coefficient calculation for the helical coil.[5]

Salimpour (2009) performed experimental investigation on the heat transfer coefficients of shell and helically coiled tube heat exchanger. He performed experiments on three heat exchangers with different pitches for both parallel-flow and counter-flow. It was found out from the experiments that the heat transfer coefficients with larger pitches are higher than those for smaller pitches. Empirical correlations were proposed for shell-side and tube-side heat transfer coefficient. [6]

J. S. Jayakumar (2010) in this study developed a correlation based on the CFD analysis results to evaluate the heat transfer coefficient in helical coil. Analysis was done for both the constant wall temperature and constant wall heat flux boundary conditions. Various numerical analyses were done to relate the coil parameters to the heat transfer. It was found that The coil parameters like the tube diameter, coil diameter have significant effect on the heat transfer and the effect of the pitch is negligible.[7]

M. Mozzafari (2015) et al conducted the experiment in order to find out the condensation and pressure drop characteristic of R600a inside a helical tube in tube heat exchanger. Experiment were conducted on different inclination angle of axis of condenser. Inclination angle of zero, $+30^0$, $+60^0$ $+90^0$ from horizontal were taken. Experiments were conducted on straight tube-in-tube condenser and inside a helical tube-in-tube heat exchanger. After conducting experiment it was found that highest value of heat transfer co- efficient occur at 30^0 and lowest value of heat transfer co- efficient occur at 90^0 inclination angel. Pressure drop has the maximum value for the horizontal case. It was found that in comparison with horizontal straight condenser, the average heat transfer and the pressure drop of the horizontal helical condenser increases. [8]

III. PROBLEM STATEMENT

Considerable experimental work has been done on helical coil of different material such as mild steel, copper etc. Few work has been reported for condensation heat transfer for stainless steel material. Helical coil made up of stainless material is fabricated and is tested under different working conditions.

(1) Impact of variable inlet temperature of steam and mass flow rate of steam on condensation heat transfer co-efficient.

IV. OBJECTIVES

I. To construct the Experimental setup to investigate the condensation of steam inside helical coil.

II. To study the effect of inlet temperature of steam on heat transfer coefficient.

V. SOLUTION PROCEDURE

Solution for the above defined problem statement can be achieved through these steps:

A Experimental setup:

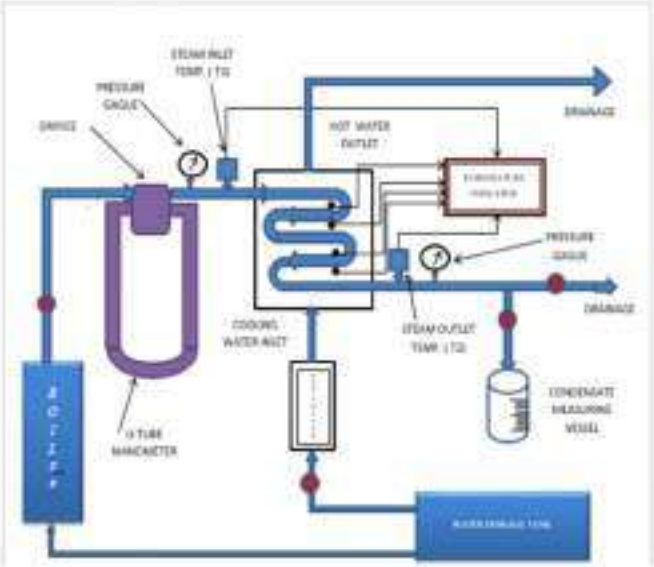

Fig 2. Shows a schematic diagram of the experimental facility. It consist of following component:

(1) Mini boiler
(2) Helical coil
(3) Test section
(4) Water storage tank

1 Mini Boiler:

It is a small size boiler capable of generating steam of pressures up to 4 kg/cm^2. It gives out dry steam at 4 bar pressure. It works on 240V, 16A power supply. It has a pressure gauge, built-in pressure regulator and safety valve in case the pressure increases beyond safe levels.

2 Helical coil:

The helical coil is made from the ¼ inch S.S seamless pipe. Three helical coils are made of coil diameter of 175, 150, and 125 mm respectively. Number of turns are 6. Pitch is kept 5mm. The axis of the coil is in the vertical direction. The steam entered the coil from the top and the condensate exited from the bottom.

3 Test section:

The tank is to be made of cylindrical mild steel vessel having diameter of 300,285, and 255mm respectively, height 250 mm. It is made from the MS sheet of 2 mm thickness by rolling the sheet in the rolling machine. The temperature of the fluid in tank is measured with the help of RTD (Resistance temperature detector). The tank has a water inlet and a water outlet valve and a valve for draining the water after experiment is performed. The inlet and outlet for water is 0.5 inch diameter pipe. One of the tubes is connected to the main water supply line and the other goes into the drain. The drainage valve given at the bottom of the tank is connected to the drain and after the experiment is performed the drain valve is opened, all the water collected inside the drum is drained. It has hole for thermocouple connection and air vent.

4 Water storage tank:

Water storage tank is used to supply the water to boiler as well as to test section

B. Instrumentation:

Following are the instrument required for experimental setup:

I. Temperature indicator:

Temperature indicator is used to indicate the surface temperature of helical coil. Multi-channel indicator is required as we need to measure the temperature across each turn of helical coil. Temperature indicator with least count of 0.1 °C is Preferred.

II. RTD (Resistance temperature indicator):

Resistance temperature detectors is used as temperature sensing element which sense the temperature of helical coil. Range of temperature sensing element required is 100-150 °C. RTD sensors are available in various forms such as rod type, rectangular type, circular type etc.

III. Rotameter:

Rotameters are used as a flow control device. This is used to control the cooling water flow rate. Range of rotameter required is 2-10 LPM.

IV. Pressure gauge:

Pressure gauges are used to measure the inlet and outlet steam pressure. Range of pressure gauge required is 0-8 Kg/cm^2.

C. Measurement and Methodology:

Boiler is operated manually, pump fitted inside the mini boiler sucks the water inside the boiler. Water is electrically heated inside the boiler at 4 kg/cm^2 pressure. Steam generated inside the boiler is allowed to pass through inlet of helical coil. Helical coil is placed inside the water tank. While passing through the helical coil steam gives its energy to surrounding cooling water. Condensate steam is collected from the outlet of helical coil. Rotameter is used to control the flow rate of

cooling water going to the tank. Experiment is carried out for different flow rate of steam.
Temperature across each turn of helical coil is measured with the help of RTD. Inlet and outlet temperature of steam is also recorded. Pressure gauges are used to record the inlet and outlet pressure of steam. Temperature of cooling water and hot water is also recorded.

VI. RESULTS AND DISCUSSION

A. Effect of inlet temperature of steam on heat transfer co-efficient for 125mm helical coil at 5 lpm of water flow rate:

Variation in heat transfer co-efficient for various inlet temperature of steam while passing through the helical coil is shown in figure.

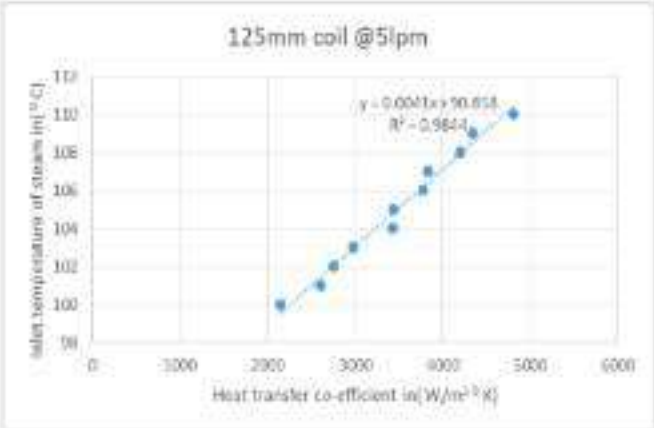

Fig 3.Variation in Heat transfer co- efficient for different mass inlet temperature of steam at 5 lpm of water flow rate.

From the above figure it is very clear that as inlet temperature of steam increasing the heat transfer co-efficient also increases.

B. Effect of inlet temperature of steam on heat transfer co-efficient for 125mm helical coil at 2 lpm of water flow rate

: Variation in heat transfer co-efficient for various inlet temperature of steam while passing through the helical coil is shown in figure.

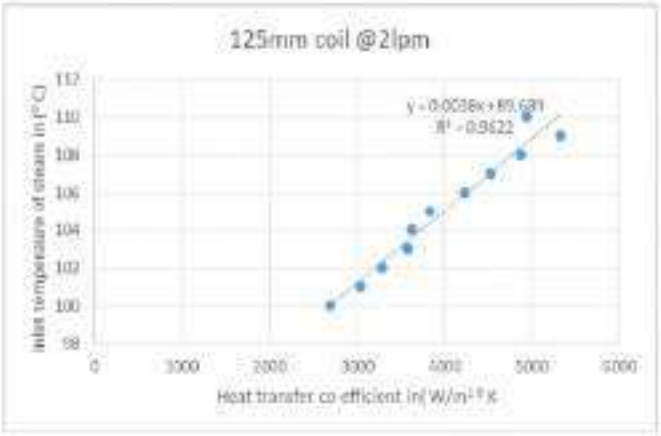

Fig 4 Variation in Heat transfer co- efficient for different mass inlet temperature of steam at 2 lpm of water flow rate.

From the above figure it is very clear that as inlet temperature of steam increasing the heat transfer co-efficient also increases.

VII. CONCLUSION

From the above figure it is very clear that heat transfer co-efficient increase with increasing inlet temperatures of steam for both 5lpm and 2lpm of water flow rate. For 5lpm the range of heat transfer co-efficient is from 2150.505 to 4806.536 (W/m^2 ^{0}K) and for 2lpm the range of heat transfer co-efficient is from 2698.278 to 4939.634 (W/m^2 ^{0}K). Therefore the range of heat transfer co-efficient for 2lpm is more compared to that of 5lpm.

REFERENCES

[1]. Tushar V. Mahale Mrinmoy D. Mallick Wasim R. Shaikh,2005, "Liquid phase heat transfer in Helical coiled heat exchanger", University of pune.
[2]. Liang Zhao, Liejin Guo , Bofeng Bai, Yucheng Hou, Xanan Zhang,2003 "Convective boiling heat transfer and two-phase flow characteristics inside a small horizontal helically coiled tubing once-through steam generator"
[3] Prabhanjan,D.G., T. J. Rennie, G.S.V. Raghavan. 2004. "Natural convection heat transfer from helical coiled tubes" International Journal of Thermal Sciences, 43(4),359-365
[4] M.H. Al-Hajeri , A.M. Koluib, M. Mosaad, S. Al-Kulaib ,2007 "Heat transfer performance during condensation of R-134ainside helicoidal tubes"
[5] Jayakumar J. S., S.M. Mahajani, J.C. Mandal, P.K. Vijayan, Rohidas Bhoi, "Experimental and CFD estimation of heat transfer in helically coiled heat exchangers", Chemical Engineering Research and Design, Volume 86, Issue 3, Pages 221-232, 2008
[6] M.R. Salimpour , "Heat transfer coefficients of shell and coiled tube heat exchangers", Experimental Thermal and Fluid Science 33 (2009) 203–207, 2009
[7] J. S. Jayakumar, "Helically Coiled Heat Exchangers, Heat Exchangers Basics Design Applications", Dr. Jovan Mitrovic (Ed.), ISBN: 978-95351-0278-62,2010.
[8] M. Mozafari, M.A. Akhavan-Behabadi, H. Qobadi-Arfaee, M. Fakoor-Pakdaman, " Condensation and pressure drop characteristics of R600a in a helical tube-in-tube heat exchanger at different inclination angles"2015